Towards Brain-Robot Interfaces in Stroke Rehabilitation

M. Gomez-Rodriguez*†, M. Grosse-Wentrup*, J. Hill*‡ A. Gharabaghi§, B. Schölkopf* and J. Peters*
*Max Planck Institute for Intelligent Systems, Tübingen, Germany
†Department of Electrical Engineering, Stanford University, CA, USA
‡Wadsworth Center, Albany, NY, USA
§Werner Reichardt Centre for Integrative Neuroscience, Eberhard Karls University Tübingen, Germany

***Abstract*—A neurorehabilitation approach that combines robot-assisted active physical therapy and Brain-Computer Interfaces (BCIs) may provide an additional mileage with respect to traditional rehabilitation methods for patients with severe motor impairment due to cerebrovascular brain damage (*e.g.*, stroke) and other neurological conditions. In this paper, we describe the design and modes of operation of a robot-based rehabilitation framework that enables artificial support of the sensorimotor feedback loop. The aim is to increase cortical plasticity by means of Hebbian-type learning rules. A BCI-based shared-control strategy is used to drive a Barret WAM 7-degree-of-freedom arm that guides a subject's arm. Experimental validation of our setup is carried out in both healthy subjects and stroke patients. We review the empirical results we have obtained to date, and argue that they support the feasibility of future rehabilitative treatments that build on this combined novel approach.**

I. Introduction

Current rehabilitation methods for patients with severe motor impairment due to cerebrovascular brain damage are limited in terms of providing long-term functional recovery. In particular, functional recovery of stroke patients beyond one year post-stroke is rare [1], and there is empirical evidence for a long-term decline of functional independence [2]. Therefore, novel rehabilitative strategies are needed.

In the last decade, many therapeutic robots and orthosis have been developed to enhance post-stroke rehabilitation of arm or hand movement and gaits (e.g., MIT-Manus [3], MIME [4], ARMin II [5], Lokomat [6], [7], Hocoma [8], etc.). Several rehabilitation robots have different modes of operation (passive, active-assisted, and active-resisted) which resulted in a promising overall effectiveness in clinical trials [9]–[12]. Nevertheless, for arm rehabilitation, the improvement in motor control of the impaired arm of stroke patients provided by robot-assisted physical therapy may not result in a consistent improvement of the functional abilities of the stroke patients [11].

Recently, alternative strategies for neurorehabilitation have been suggested which are based on decoding of motor imagery with a Brain-Computer Interface (BCI). Such motor imagery decoding has been demonstrated to be feasible in chronic stroke patients [13]. More importantly, these strategies have exhibited beneficial effects on the restoration of basic motor functions in stroke patients [14], [15].

The logical next step combines robot-assisted physical therapy with BCI-based motor imagery decoding into an integrative rehabilitation strategy. In such an integrative therapy, it is essential that patients exert control over their robot-assisted physical therapy. This step requires that a BCI system decodes the movements intention of the patient. Here, a continuous synchronization is required between the subject's motor imagery or movement attempt and the actual movement of the robot that guides the subject's impaired limb. Such synchronization stands in contrast to previous studies where haptic feedback was provided at the end of each trial [16]. It is likely to result in an increased cortical plasticity due to Hebbian-type learning [17]–[19], and has the potential to improve the functional recovery.

In this paper, we present the combined BCI-robotics system developed for this purpose at the Max Planck Institute for Intelligent Systems. We drive a Barrett WAM 7 degree-of-freedom (DoF) arm (which has been attached to the subject's impaired arm) using a EEG- or ECoG-based BCI shared-control strategy. To achieve a high classification accuracy also with EEG, we aim to decode only (one-dimensional) movement intentions or attempts of pre-defined trajectories and do not focus on the alternative of decoding multiple DoF from ECoG recordings [21]. Decoding a single DoG, we can achieve not only high classification accuracy but also small delays in the feedback loop. It is likely that these properties are more important for inducing cortical plasticity than movement complexity. We employ on-line signal processing and machine learning methods to decode the recorded neural signals. The WAM arm provides haptic feedback and it implements three different modes of operation: *passive*,

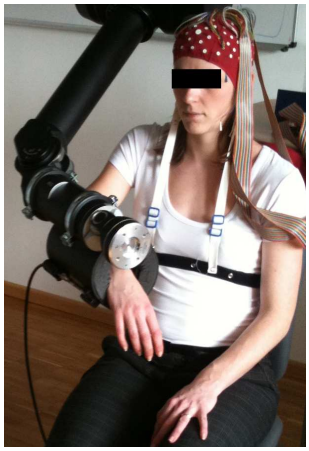

Fig. 1. A robot arm is attached to the patient's forearm and it may move the patient's forearm with the elbow as the single degree of freedom (DoF). The resting position, maximum extension and maximum flexion of the robot arm can be adjusted depending on the patient (adapted from [20]).

autonomous active, and *subject-driven passive-active* mode (see Section II for a discussion on the modes of operations of the robot arm).

The paper is organized as follows. Section II is devoted to our approach for Brain-Robot Interfaces in neurorehabilitation, including a description of the basic BCI setup, the modes of operation of the Barrett arm and our resulting strategy. In Section III, we review the empirical results we have obtained to date with healthy subjects as well with stroke patients. The paper concludes with a discussion and a summary of the presented ideas in Section IV.

II. A BCI-BASED REHABILITATION ROBOTICS SETUP

Heading towards the goal of a framework for brain-robot interfaces for stroke rehabilitation, we need to connect a brain-computer interface with a robot in a manner that the resulting haptic feedback benefits the patient. This part requires the existence of a BCI interface that continuously adapts to the patient and learns online how to decode his or her movement intention. See Section II-A for signal processing of the recorded neural signals. A brain-robot interface obviously also requires that the decoded movement intention is fed back to the patient using the robot as haptic display either in a passive mode, an autonomous active mode or a patient-driven passive-active mode (see Section II-B). The monitored movement, force and neural signals are finally used in a basic strategy for rehabilitation sessions as described in Section II-C.

A. On-line Learning of Movement Intention with a BCI

A key step in the setup is the online decoding of the movement intention of the system. This step requires collection and pre-processing of neural signals as well as continuous online adaptation of the movement intention classification.

The system relies on either EEG or ECoG to collect neural signals. The sampled signals are subsequently preprocessed using a centre-surround spatial sharpening filter or *surface Laplacian* [22] as well as a band pass filter. The signals are processed into 20 online features per electrode by discretizing the normalized average power spectral densities into 2 Hz frequency bins in the frequency range (2–42 Hz), as previously used in motor imagery with EEGs [23]. Welch's method is used to compute an estimate of the power spectral density (PSD). In each movement or resting period, the first PSD estimate is computed using 500ms and from that moment on every 300 ms, allowing an on-line classification every 300ms.

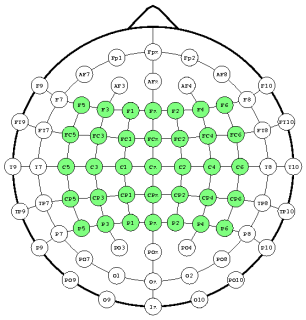

Fig. 2. EEG electrode grid configuration in our experiments. The relevant electrodes are shown in green covered parts of the pre-motor cortex, primary motor cortex and somatosensory cortex (adapted from [20]).

The online decoding decides between three movement intentions of the patient, i.e., flexion, resting and extension, using the features described above. On-line classification is achieved by discriminating flexion vs resting, and extension vs resting. Two linear support vector machine (SVM) classifiers [24] are generated on-the-fly after a training section. The generation of training data is part of the rehabilitation robotics strategy and described in detail in Section II-C.

B. Haptic Interaction with a Robot Arm

Smart haptic feedback based on decoded movement intention would set a novel stroke rehabilitation approach based on a brain-robot interface apart from previous ones. A haptic reinforcement is likely to result into improved performance over a pure robotics setting or a pure motor imagery one. Few robots allow achieving sufficient performance for such robot-based haptic display. A backdrivable low friction robot arm with low-level torque control is needed, such as the WAM robot arm made by Barrett Technology Inc. On this robot arm, we could implement three different modes of haptic interaction, i.e., passive, autonomous active and patient-driven passive-active. In all modes of operation, the subject can be instructed either to try to perform a flexion or extension or to perform motor imagery (also flexion or extension).

In the *passive mode*, the patient is instructed to either attempt arm flexion or arm extension or motor imagery while the robot arm tracks the position and velocity of the patient's movement. When the patient is instructed to attempt a real movement, the relevant DoFs of the robot arm are set in a compliant mode where the external forces such gravity are compensated for. At the same time, all other joints are fixed to a comfort posture customized to the individual patient. During motor imagery, *all* the joints are fixed to this comfort posture. Note that when the robot compensates the gravity of the elbow joint to perform a flexion, it blocks the elbow joint in the direction of an extension, and for an extension, it blocks the joint in the direction of a flexion. This block helps the patient during the movement attempt.

The robot arm performs an active flexion or extension of the elbow joint, guiding the patient's owns movement, while all the other joints are fixed to an arbitrary (customizable) position. This setting is called *autonomous active mode* where the patient is instructed either to attempt to follow the robot arm's active movement or to perform motor imagery that mimics the movement of the robot arm.

In a *patient-driven passive-active mode*, the Brain-Robot Interface decodes every 300ms whether the patient is attempting to perform an arm movement (flexion or extension) or perform motor imagery based on the neural signals coming from an EEG- or ECoG-based BCI. Therefore, every 300ms the state of the robot arm is updated to active movement (flexion or extension) or resting. If the robot is in active moment state, it performs an active flexion or extension of the elbow joint. If the robot is in resting state and the patient is instructed to attempt real movements, it switches to compliant mode (i.e., gravity compensation), as in the passive mode, allowing the

patient to move the arm actively. If the robot is in resting state but the patient is instructed to perform motor imagery, the elbow joint is fixed to the current position. As in the previous modes, all the other joints are fixed to an arbitrary (customizable) position. This mode requires a neural classifier of movement attempt or intention vs rest (see Section II-C for a description of a rehabilitation session, which explains how the classifier is trained). Finally note that, by this mode, we are providing haptic feedback.

The speed, torques and maximum ranges used by the robot when moving actively or fixing a position are customizable in our setup. In addition, in all modes, when the patient's reaches a maximum range of extension or flexion, or a time limit is reached, the robot guides actively the patient's arm to the initial position.

Note that the haptic feedback in the last mode of operation is given in a synchronized manner with the subject's attempt to move the arm or the motor imagery, and not at the end of a trial as done previously [16]. Moving the robot throughout each trial, and not at the end of it, is a key point in terms of a future neurorehabilitation therapy, because it is a strategy that is likely to result in increased cortical plasticity due to Hebbian-type learning [17]–[19].

C. Resulting Rehabilitation Robotics Strategy

Our framework monitors the position and velocity of the elbow joint of the Barrett arm and the EEG- or ECoG-based neural activity of the patient throught the rehabilitation session. This enables the real-time as well as off-line analysis of correlations between movement performance and neural signals.

A rehabilitation session with our Brain-Robot Interface is divided into blocks. A block is a collection of an arbitrary number of consecutive trials separated from each other by a pause of a few seconds. In each trial, the patient is instructed to either attempt to perform flexion or extension of the forearm or perform motor imagery of the forearm (also flexion or extension), using the elbow joint as the single degree of freedom (see Figure 1). A trial is divided into three consecutive phases. Each trial starts with the instruction "Relax". Then, patients are cued on the upcoming type of motor imagery ("Flexion" or "Extension"), and later on, they are instructed to initiate either the movement attempt or the motor imagery by a "Go"-cue. This phase of movement attempt or motor imagery lasts either until the arm hits its maximum range or a maximum time is achieved. Cues are delivered visually as text displayed on a computer screen. In addition, each textual cue is spoken out loud as an auditory cue. For a better understanding, Figure 3 illustrates the timeline of events during one trial.

A block is divided in two consecutive sections, a training section and a test section. The training section lasts an arbitrary number of trials and it aims to provide enough amount of neural recordings for each type of movement (*i.e.*, flexion and extension) and for rest. Note that the data for each type of movement and rest are not collected in a consecutive manner but in each period of movement and rest. The test section lasts the remaining number of trials following the training section.

During the training section, only the first two modes of operation of our Brain-Robot Interface (i.e., passive and autonomous active modes) can be used, as no neural classifier is yet trained. In the test section, any of the three modes of operation (i.e., passive, autonomous active and patient-driven passive-active) can be used. See Section II-B for a description of the modes of operation of our Brain-Robot Interface. In addition, during the test section, visual feedback is given in form of an arrow on the computer screen during the movement periods. At the beginning of the movement period of each trial, the arrow is located in the center of the screen and its position is updated every 300ms according to the decoded movement intention.

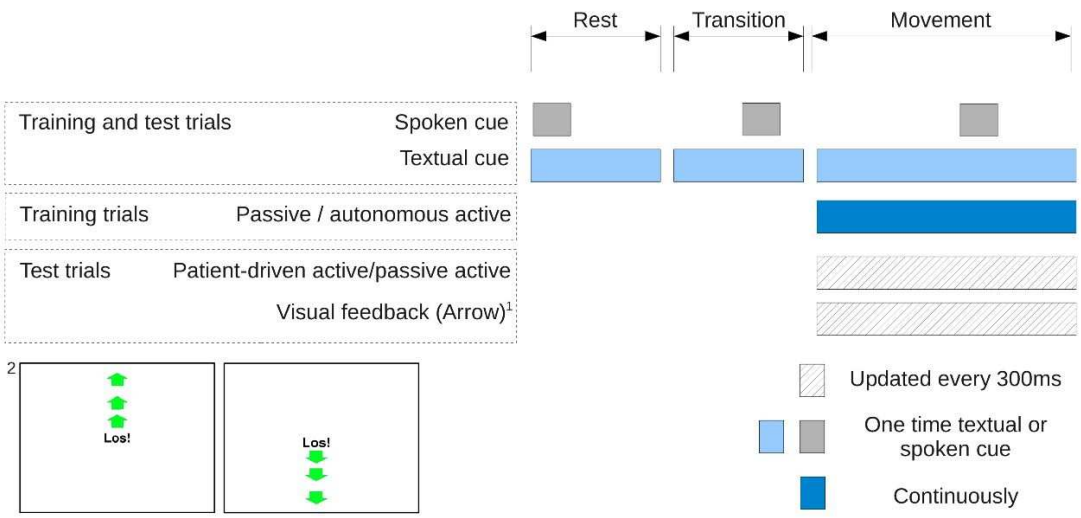

Fig. 3. Timeline of events in a single trial. Please note that the spoken and textual cues are one-time events. For movement periods of training sections, the movement of the robot is continuous, while for movement periods of test sections, the haptic and visual feedback are events that are updated every 300ms (adapted from [20]).

III. Feasibility Evaluation and Experiments

We have evaluated our Brain-Robot Interface in a feasibility study with six right-handed healthy subjects and three right-handed stroke patients with a hemiparesis of the left side of their body using an 35-electrode EEG-based BCI module (see Figure 2 for electrode grid spatial configuration) [20]. Here, we review these experimental results. First, we show the position of the elbow joint for one of the stroke patients (performing an impaired real movement) for all modes of operation. Later

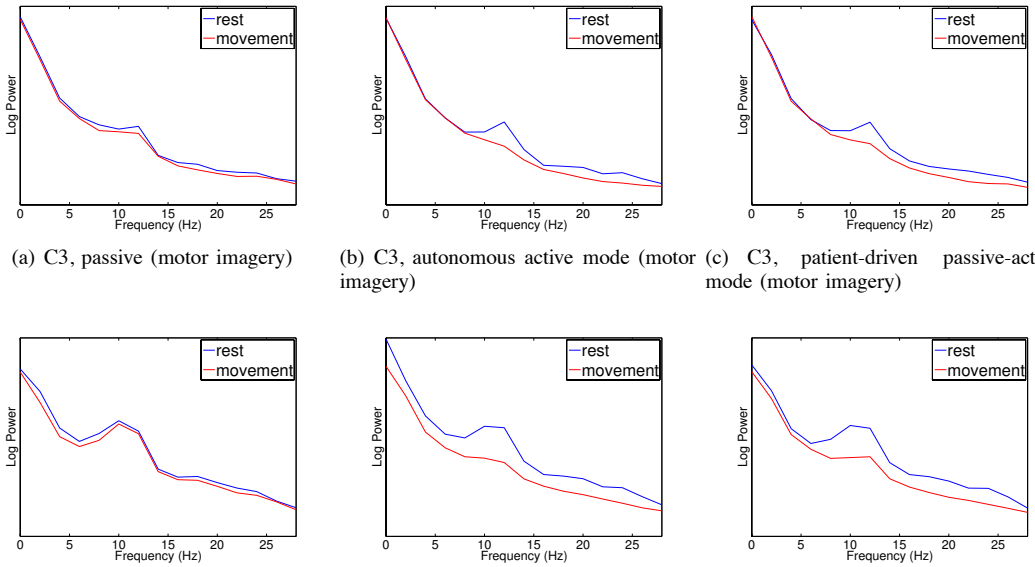

(a) C3, passive (motor imagery)

(b) C3, autonomous active mode (motor imagery)

(c) C3, patient-driven passive-active mode (motor imagery)

(d) CP3, motor imagery (motor imagery)

(e) CP3, autonomous active mode (motor imagery)

(f) CP3, patient-driven passive-active mode (motor imagery)

Fig. 4. **Power spectra of the electrodes C3 and CP3 for healthy subjects**: Power spectra in movement periods and the rest periods for the electrodes C3 and CP3 in the frequency band 2–30 Hz for motor imagery (i.e., no robot neither real movement), the autonomous active mode and the patient-driven passive-active mode (adapted from [20]).

on, we discuss the powerspectra of two electrodes that lie over the motor and somatosensory area (C3 and CP3) for six healthy subjects (performing motor imagery) and all modes of operation. Finally, also in healthy subjects, we compare the spatial and spectral distribution of classifier weights of training periods in which the robot is in autonomous active mode and of training periods in which the robot is in passive mode.

Figure 5 shows the position and velocity of the elbow joint for the different modes of operation during one run with one of the stroke patients. We observe empirical evidence of the following facts. First, both for the autonomous and the patient-driven passive-active mode, the elbow joint reaches the maximum range in a larger number of cases than for the passive mode, in which the patient attempts to perform the arm movement only with the help of gravity compensation. Second, the movement is smoother in the patient-driven passive-active mode than in the passive mode – the robot arm active movement establishes a uniform pace for the patient to follow. Third, when in compliant mode (i.e., gravity compensation), there is a faster drop at the beginning of a movement period in which a flexion is attempted. This occurs because the robot arm was heading to the floor and therefore the gravity compensation makes the robot arm drop in absence of any force.

Figure 4 shows the power spectra per frequency bin for the electrodes C3 and CP3 for the passive mode, autonomous active mode and the patient-driven passive-active mode for six healthy subjects that are instructed to perform motor imagery (flexion or extension). We observe a bigger ERD/ERS modulation for both the autonomous active and patient-driven passive-active modes in comparison with motor imagery, i.e., when the robot is moving the subject's arm, the desynchronization is stronger.

Figure 6 shows the classifier weights per electrode averaged over the frequency bands 8–16 Hz and 18–28 Hz on a group level for the healthy subjects. Note that healthy subjects were instructed to perform motor imagery of the right forearm. We observe empirical evidence of the following facts. First, electrodes over the motor area representing the right arm, *i.e.*, C3, CP3, FC3, FC1, ..., get larger weights (*i.e.*, have a higher discriminative power) when the robot arm is in autonomous active mode (i.e., it guides the subject's arm during the training period) in both frequency bands. Second, there is a higher discriminative power of the sensorimotor area during training periods in which the robot arm is in autonomous active mode for the frequency band that contains the β rhythm. Third, the spatial distribution of the weights in the classifiers indicates that the classifiers employed neural activity, as the weights in the peripheral locations are low. Hence, it is not likely that electromyographic (EMG) activity coming from movements of the head or the face plays a major role.

Figure 7 shows the average classifier weights per frequency bin for the electrodes C3, CP3 and C4. We observe a shift in discriminative power towards higher frequencies, *i.e.*, from μ rythm desynchronization to β rythm desynchronization, for training periods in which the autonomous active mode is used.

IV. Discussion and Conclusion

In this paper, we have introduced a Brain-Robot Interface for neurorehabilitation that artificially supports the sensorimotor feedback loop. The additional mileage of our system with

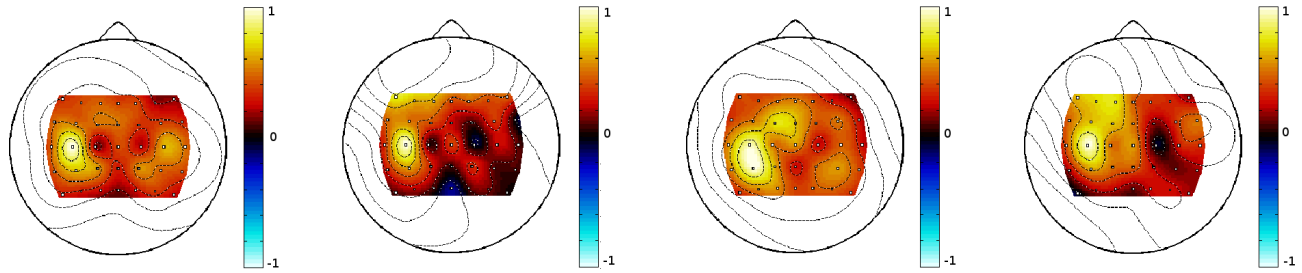

(a) 8–16 Hz, autonomous active (b) 8–16 Hz, passive (c) 18–28 Hz, autonomous active (d) 18–28 Hz, passive

Fig. 6. **Discriminative power of the electrodes for healthy subjects**: Comparison of the classifier weights for the frequency bands (a,b) 8–16 Hz and (c,d) 18–28 Hz, between the autonomous active mode (a,c) and the passive mode (b,d) (adapted from [20]).

respect to previous work [16] is provided by the following characteristic of our system. First, there is a synchronization of the subject's intention or attempt with the actual movement of the robot that guides the subject's impaired limb, not as in previous studies in which haptic feedback was provided at the end of each trial. This synchronization is likely to result in an increased cortical plasticity due to Hebbian-type learning rules [17]–[19], potentially resulting in an improvement of the functional recovery. Second, our system supports both subject's motor imagery and subject's real movement, given that it is not yet clear what is the optimal strategy for neurorehabilitation. Third, our system enables simultaneous monitoring of positions and velocities of the elbow joint and neural signals, and this will enable future research work and rehabilitation strategies based on the correlations between real movement performance and neural content.

The beneficial effect of our rehabilitation framework is likely to depend on the presence of proprioception. However, there is no a-priori reason why stroke patients should not have proprioception. All stroke patients in our studies had intact proprioception, and previous studies have shown that most stroke patients recover proprioception eight weeks post-stroke despite remaining motor disabilities [25].

Besides the relevance of our rehabilitation framework for a potential stroke therapy, our strategy may also be beneficial for other subject groups. For example, subjects in late stages of ALS appear not to be capable of modulating their SMR sufficiently, as indicated by fact that so far no communication with a completely locked-in subject has been established by means of a BCI. While the extent of sensory feedback in late stages of ALS remains unclear, haptic feedback might also support these subjects in initiating volitional modulation of their SMR.

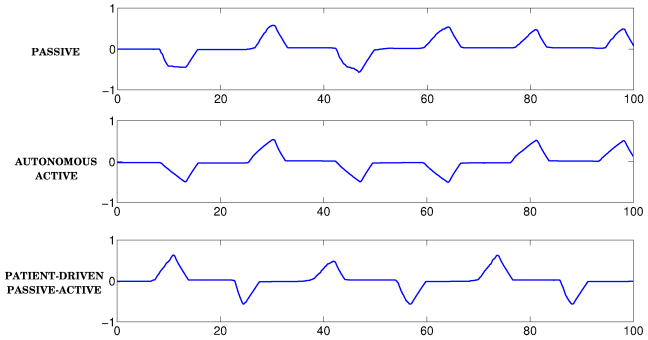

Fig. 5. Position of the elbow joint for all three modes of operation of our Brain-Robot Interface. Horizontal axis indicates time (in seconds), and vertical axis indicates position of the elbow joint (in radians).

References

[1] M. Johnston, B. Pollard, V. Morrison, and R. MacWalter. Functional limitations and survival following stroke: psychological and clinical predictors of 3-year outcome. *International journal of behavioral medicine*, 11(4):187–196, 2004.

[2] M.S. Dhamoon, Y.P. Moon, M.C. Paik, B. Boden-Albala, T. Rundek, R.L. Sacco, and M.S.V. Elkind. Long-term functional recovery after first ischemic stroke: the Northern Manhattan Study. *Stroke*, 40(8):2805, 2009.

[3] H.I. Krebsa, N. Hogana, B.T. Volpec, M.L. Aisend, L. Edelsteine, and C. Dielse. Overview of clinical trials with MIT-MANUS: a robot-aided neuro-rehabilitation facility. *Technology and Health Care*, 7(6):419–423, 1999.

[4] C.G. Burgar, P.S. Lum, P.C. Shor, and H.F.M. Van der Loos. Development of robots for rehabilitation therapy: The Palo Alto VA/Stanford experience. *Journal of Rehabilitation Research and Development*, 37(6):663–674, 2000.

[5] M. Mihelj, T. Nef, and R. Riener. Armin ii - 7 dof rehabilitation robot: mechanics and kinematics. In *Robotics and Automation, 2007 IEEE International Conference on*, pages 4120 –4125, 2007.

[6] B. Husemann, F. Muller, C. Krewer, S. Heller, and E. Koenig. Effects of locomotion training with assistance of a robot-driven gait orthosis in hemiparetic patients after stroke: a randomized controlled pilot study. *Stroke*, 38(2):349, 2007.

[7] A. Mayr, M. Kofler, E. Quirbach, H. Matzak, K. Fröhlich, and L. Saltuari. Prospective, blinded, randomized crossover study of gait rehabilitation in stroke patients using the Lokomat gait orthosis. *Neurorehabilitation and Neural Repair*, 21(4):307, 2007.

[8] J. Hidler, D. Nichols, M. Pelliccio, and K. Brady. Advances in the understanding and treatment of stroke impairment using robotic devices. *Topics in stroke rehabilitation*, 12(2):22–35, 2005.

[9] R.P.S. van Peppen, G. Kwakkel, S. Wood-Dauphine, H.J.M. Hendriks, Ph.J. van der Wees, and J. Dekker. The impact of physical therapy on functional outcomes after stroke: what's the evidence? *Clinical Rehabilitation*, 18(8):833–862, 2004.

[10] R. Riener, T. Nef, and G. Colombo. Robot-aided neurorehabilitation of the upper extremities. *Medical and Biological Engineering and Computing*, 43(1):2–10, 2005.

[11] G.B. Prange, M.J.A. Jannink, C.G.M. Groothuis-Oudshoorn, H.J. Hermens, and M.J. IJzerman. Systematic review of the effect of robot-aided therapy on recovery of the hemiparetic arm after stroke. *Journal of Rehabilitation Research and Development*, 43(2):171, 2006.

[12] G. Kwakkel, B.J. Kollen, and H.I. Krebs. Effects of robot-assisted therapy on upper limb recovery after stroke: a systematic review. *Neurorehabilitation and Neural Repair*, 22(2):111, 2008.

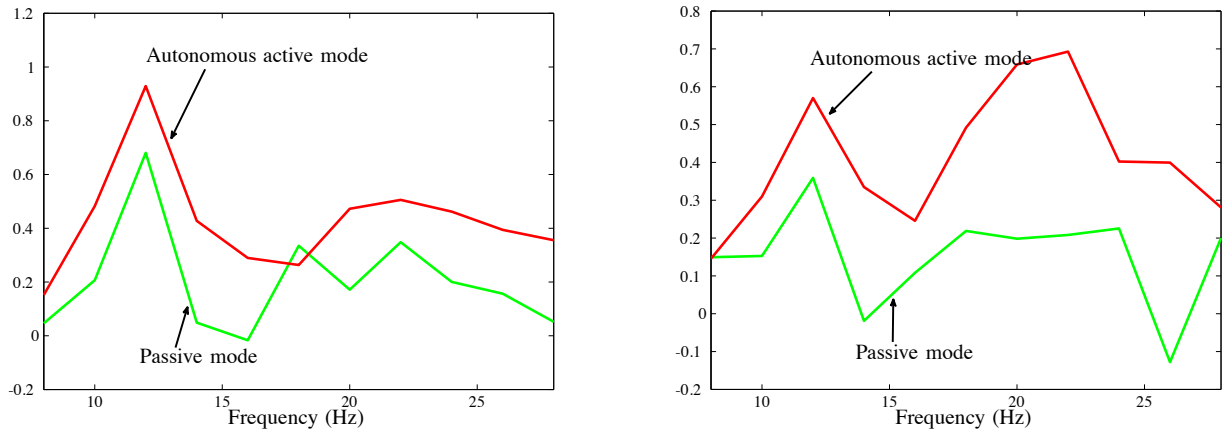

(a) Classifier weights for electrode C3

(b) Classifier weights for electrode CP3

Fig. 7. **Discriminative power of the frequency components of the electrodes C3 and CP3 for healthy subjects**: Classifier weights for the electrodes C3 and CP3 in the frequency band 8–30 Hz for for training periods in which the autonomous active mode and the passive mode are used (adapted from [20]).

[13] E. Buch, C. Weber, L.G. Cohen, C. Braun, M.A. Dimyan, T. Ard, J. Mellinger, A. Caria, S. Soekadar, and A. Fourkas. Think to move: a neuromagnetic brain-computer interface (bci) system for chronic stroke. *Stroke*, 39(3):910, 2008.

[14] H.C. Dijkerman, M. Ietswaart, M. Johnston, and R.S. MacWalter. Does motor imagery training improve hand function in chronic stroke patients? A pilot study. *Clinical Rehabilitation*, 18(5):538, 2004.

[15] S.J. Page, P. Levine, and A. Leonard. Mental practice in chronic stroke: results of a randomized, placebo-controlled trial. *Stroke*, 38(4):1293, 2007.

[16] K.K. Ang, C. Guan, S.G. Chua, B.T. Ang, C. Kuah, C. Wang, K.S. Phua, Z.Y. Chin, and H. Zhang. A clinical study of motor imagery-based brain-computer interface for upper limb robotic rehabilitation. In *Annual International Conference of the IEEE Engineering in Medicine and Biology Society (EMBC)*, pages 5981–5984, 2009.

[17] W. Wang, J.L. Collinger, M.A. Perez, E.C. Tyler-Kabara, L.G. Cohen, N. Birbaumer, S.W. Brose, A.B. Schwartz, M.L. Boninger, and D.J. Weber. Neural Interface Technology for Rehabilitation: Exploiting and Promoting Neuroplasticity. *Physical Medicine and Rehabilitation Clinics of North America*, 21(1):157–178, 2010.

[18] T.H. Murphy and D. Corbett. Plasticity during stroke recovery: from synapse to behaviour. *Nature Reviews Neuroscience*, 10(12):861–872, 2009.

[19] L. Kalra. Stroke Rehabilitation 2009: Old Chestnuts and New Insights. *Stroke*, 41(2):e88, 2010.

[20] M. Gomez-Rodriguez, J. Peters, J. Hill, B. Schölkopf, A. Gharabaghi, and M. Grosse-Wentrup. Closing the sensorimotor loop: haptic feedback facilitates decoding of motor imagery. *Journal of Neural Engineering*, 8(036005), 2011.

[21] T. Pistohl, T. Ball, A. Schulze-Bonhage, A. Aertsen, and C. Mehring. Prediction of arm movement trajectories from ECoG-recordings in humans. *Journal of Neuroscience Methods*, 167(1):105–114, 2008.

[22] D.J. McFarland, L.M. McCane, S.V. David, and J.R. Wolpaw. Spatial filter selection for EEG-based communication. *Electroencephalography and Clinical Neurophysiology*, 103(3):386–394, 1997.

[23] M. Grosse-Wentrup, C. Liefhold, K. Gramann, and M. Buss. Beamforming in noninvasive brain-computer interfaces. *IEEE Transactions on Biomedical Engineering*, 56(4):1209–1219, 2009.

[24] B. Schölkopf and A.J. Smola. *Learning with kernels: Support vector machines, regularization, optimization, and beyond*. the MIT Press, 2002.

[25] D.L. Smith, A.J. Akhtar, and W.M. Garraway. Proprioception and spatial neglect after stroke. *Age and Ageing*, 12(1):63, 1983.